ExpeER

Distributed Infrastructure for EXPErimentation in Ecosystem Research

Grant Agreement Number: 262060

SEVENTH FRAMEWORK PROGRAMME

Capacities

Integrating activities: Networks of Research Infrastructures (RIs)

Theme: Environment and Earth Sciences

DELIVERABLE D7.1

Deliverable title: Report on testing of wireless sensor networks and cosmic ray probes for field scale soil moisture assessment

Abstract: This report describes the potential of cosmic ray probes for the assessment of soil moisture at the field scale.

Due date of deliverable: M24

Actual submission date: M28

Start date of the project: December 1st, 2010

Duration: 48 months

Organisation name of lead contractor: UFZ

Contributors: Heye Bogena, Sander Huisman

Revision N°: Final version

Dissemination level:

PU Public (must be available on the website)	**X**
PP Restricted to other programme participants (including the Commission Services)	
RE Restricted to a group specified by the consortium (including the Commission Services) (precise to whom it should be addressed)	
CO Confidential, only for members of the consortium (including the Commission Services)	

Table of Content

1 Executive summary

Up to date, results from Cosmic Ray Probe (CRP) measurements are mainly presented from test sites located in high altitudes (Desilets et al., 2010) and from an agricultural fields with sandy soils (Rivera Villarreyes et al., 2011). All these studies either use gravimetric soil moisture determination from a few field campaigns or continuous data from a few classical soil moisture sensors to quantify the agreement with SWC derived from the CRP.

In this study data from the wireless soil moisture sensor network (SoilNet) providing continuous soil water content measurements at 93 locations within the footprint of the CRP, is used to investigate whether the cosmic ray method can also be applied to less favourable areas like a spruce forest site with a litter layer.

2 Theorie

2.1 Cosmic rays

Cosmic radiation can be divided in primary cosmic rays that originate from space or the sun and secondary cosmic rays generated by interaction with matter in the atmosphere or the top few meters of the earth's crust. The primary cosmic radiation consists of ~90% protons, ~9% α-particle and ~1% heavier nuclei. Nearly all primary cosmic rays that reach the earth's atmosphere are from outside the solar system, but from within the galaxy [Gaisser, 1990]. Supernova explosions and supernova remnants are the main origin for galactic cosmic rays, with an energy spectrum of 10^6 – 10^7 GeV, whereas the sun's corona produces solar cosmic rays with energies of 10 – 30 GeV during solar flares [Dorman 2004].

Solar cosmic rays are caused by sporadic, individual events, whereas galactic cosmic rays come in permanently. Nevertheless, galactic cosmic rays underlie temporal fluctuations caused by the magnet field of the heliosphere, the so called solar modulation. When the sun has many spots, its magnetic field is strong. In this case, the charged primary cosmic ray particles are deflected and the cosmic ray intensity at the earth is reduced. In addition, cosmic rays of lower energies are deflected to a stronger degree which leads not only to changes in cosmic ray intensity but also to a shift in the cosmic ray energy spectrum [Parker, 1965].

The charged protons making up the primary cosmic ray flux need to possess enough energy to penetrate the earth's magnetosphere in order to reach earth. The minimum energy needed is determined by the rigidity (momentum-to-charge ratio) cutoff of the geomagnetic field, which generally increases with decreasing latitude but nevertheless underlies fluctuations [Desilets and Zreda, 2001].

When a primary cosmic ray particle has enough energy to penetrate the atmosphere it collides with atmospheric nuclei, generating a cascade of secondary cosmic rays, mainly consisting of neutrons [Lal & Peters, 1967]. Those neutrons are produced by two kinds of interactions:

- The so called knock-out neutrons are directly knocked out of a nucleus by an incoming proton or neutron and they possess energies of ~1MeV up to the energy of the incoming particle.

- The second neutron source is the emission of evaporation neutrons, which result from a de-excitation reaction of the initially excited nucleus, mainly nitrogen and oxygen. Those evaporation neutrons are in the energy spectrum of about 1 – 2MeV.

The ratio between knock-out and evaporation neutrons is ~ 1:4 [Hess et al.,1961; Hendrick & Edge, 1966]. Each high-energy collision in the atmosphere produces 3 – 8 neutrons with an average energy of 1MeV [Phillips et al., 2001]. Cosmic rays are attenuated in exponential proportion to the cumulative mass traversed through the atmosphere or solid earth [Lal, 1991]. Therefore, the flux density of neutrons increases with increasing altitude.

High-energy neutrons travelling through the atmosphere are adsorbed or moderated (attenuated), thus creating neutrons with lower energies. The flux of neutrons with a particular energy is therefore strongly dependent on the composition of the medium traversed [Phillips et al., 2001]. The secondary neutrons are generally classified by their energies [Krane, 1988], as

- thermal: ~0.025eV
- epithermal: ~1eV
- slow: ~1keV
- fast: ~100keV-10MeV

With decreasing energy, the chance for absorption increases [Phillips et al., 2001]. Neutrons that are not absorbed will be moderated until they reach the thermal energy level, where the kinetic energy is dictated by the environment temperature (for the earth: ~0-0.5eV). Neutrons in the thermal state cannot be moderated anymore and will eventually be adsorbed by nuclei [Hendrick and Edge, 1966]. Some secondary neutrons produced in the top few meters of the soil will be able to leave the soil. They will collide with near-surface nuclei and cause further randomized particle paths until the thermal energy range is reached.

According to Zreda et al. [2012] the moderation of neutrons depends on 3 factors:

- The probability of scattering by different elements, characterized by their elemental scattering cross-section, and the associated macroscopic scattering cross-section of the material,
- The energy loss per collision or, equivalently, the number of collisions necessary to thermalize a fast neutron,
- The number of nuclei of different elements, or the elemental concentration

Since collisions with heavy nuclei transfer little energy, hydrogen is by far the best neutron moderator (Zreda et al., 2012). Hydrogen atoms in the soil, which are mainly present as water, moderate the secondary neutrons on the way back to the surface. Therefore, fewer neutrons reach the surface in moist soils, whereas under drier conditions more neutrons are able to escape the soil. This fact enables the use of the CRP to detect soil moisture.

3 Materials and Methods

3.1 The Wüstebach test site

This study was undertaken in the Wüstebach catchment, which is a small subcatchment of the Rur River and part of the TERENO Eifel/Lower Rhine Valley Observatory [Zacharias et al., 2011]. The test site is located in the German low mountain ranges within the National Park Eifel (50°30' N, 6° 19' E, WGS84) near the German-Belgian border (see Figure 1).

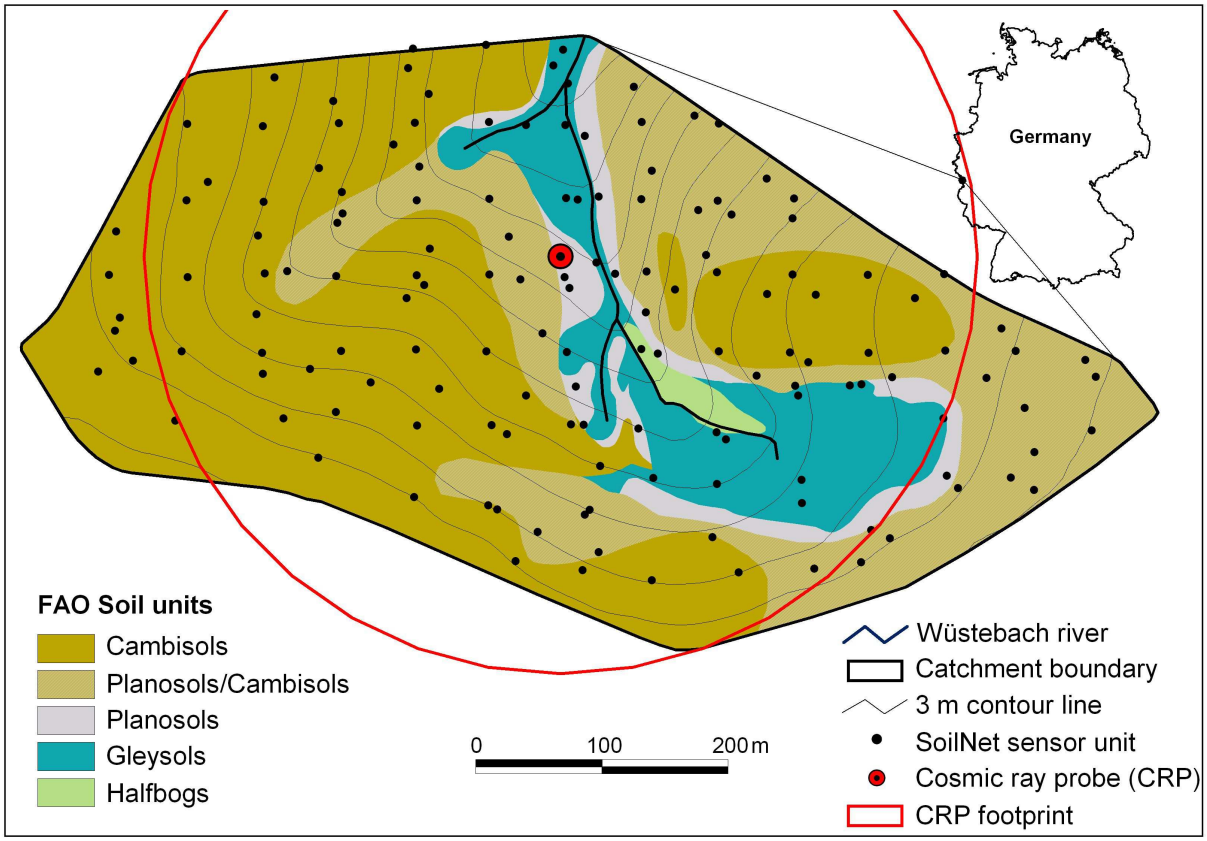

Figure 1 Location of the Wüstebach experimental test site

The Wüstebach test site covers an area of ~27ha, with altitudes ranging from 595m a.s.l. in the northern part to 628m a.s.l. in the south. The average slope is 3.6% with a maximum of 10.4%. The geology is dominated by Devonian shales with occasional sandstone inclusions, which is covered with a periglacial solifluction layer of about 1–2 m thickness. Mainly Cambisols (western part) and Planosols/Cambisols (eastern part) have developed on the hillslopes, whereas Planosols, Gleysols and half-bogs have formed under the influence of groundwater in the valley (Fig. 1). The soil texture is silty clay loam with medium to very high fraction of coarse material and the litter layer has a thickness between 3 and 5 cm [Richter, 2008]. The mean annual precipitation at the test site is about 1220mm (1979-1999) [Bogena et al., 2010]. Norway Spruce (*Picea abis L.)*, planted in 1946, is the prevailing vegetation type (~90%) [Etmann 2009].

Figure 2: The cosmic ray probe located in the Wüstebach test site.

The cosmic ray probe was mounted on a pole (50°30'12.38" N, 6°19'59.32" E, WGS84) about 1.2 m above the ground (see Fig. 2). Precipitation and atmospheric pressure were measured hourly at the nearby climate station Kalterherberg operated by the German Weather Service. The monitoring period analyzed in this study started on February 1, 2011 and ended on October 31, 2012.

3.2 The wireless sensor network SoilNet

The SoilNet is a wireless sensor network (WSN) developed at the Forschungszentrum Jülich. It enables the measurement of SWC pattern dynamics in small catchments (0.1 to several km^2) [Bogena et al. 2010]. The SoilNet consists of three basic components. First, the coordinator enables the long-distance data transmission of the measured values (e.g. via GSM modem) and initiates the wireless link within the network. Second, sensor units are deployed in the soil, measure the SWC, and transmit the data to the nearest router. Finally, routers pass the measured data from the sensor units to the coordinator. Wireless sensor networks have the advantage that the sensors remain in the exact same position, so that the measured values are not affected by small-scale spatial variability of the soil, in contrast to measurements from field campaigns. The main disadvantage of wireless networks is the power supply restriction. However, using low-current sensors, the batteries have a lifetime of a few years. Nevertheless, the power consumption of the network has to be optimized to minimize maintenance. For that purpose, SoilNet uses the license-free protocol stack JenNet, based on IEEE 802.15.4 (250kbit s^{-1}) specifications, for short-range wireless network applications [Bogena et al., 2010].

For the SoilNet application in the Wüstebach test site, ECH_2O EC-5 and ECH_2O 5TE sensors (Decagon Devices, Pullman, WA, USA) were used, which were evaluated by Rosenbaum et al. [2010] and considered appropriate for WSN applications. The calibration procedure is described in Rosenbaum et al. [2012]. The SoilNet in Wüstebach consists of 150 sensor units, where in total 600 ECH_2O EC-5 and 300 ECH_2O 5TE sensors are buried in 3 depth (5 cm, 20 cm, 50 cm), with 2 sensors in each depth, measuring every 15 minutes. Fifty sensor units are located in a 60*60 m raster, the remaining 100 are distributed randomly to enable geostatistical analysis [Bogena et al. 2010] (Fig. 1).

3.3 The cosmic ray soil moisture probe

The CRS-1000 Cosmic Ray Soil Moisture Probe (Hydroinnova LLC, Albuquerque, NM, USA) measures neutron counts at hourly interval. The main system components are two detector tubes, two pulse modules, a data logger with Iridium modem and sensors for temperature,

atmospheric pressure and relative humidity. The detector tubes mainly respond to neutrons in the thermal energy range. In order to detect neutrons in the fast energy range, one detector tube is shielded with polyethylene that moderates fast neutrons to thermal neutrons before they enter the detector tube. The tubes are filled with 3He, which has a high neutron absorption cross section, and a potential of ~1000V between the tube wall (cathode) and a thin wire in the center of the tube (anode) is applied. Neutrons entering the tube and hitting a ^{3}He atom produce several electrons which are deposited at the anode. They induce a pulse of electrical current to the pulse module, which amplifies, shapes and identifies the current as being caused by a neutron. The number of counts per hour is sent to the data logger, where it is sent to a remote desktop with an integrated Iridium modem [Zreda et al., 2012].

According to Desilets et al. [2010], the count rate can be related to soil water content by

$$\theta = a_0 \left(\frac{N}{N_0} - a_1\right)^{-1} - a_2 \qquad \text{Eq. (1)}$$

where θ is the gravimetric SWC, N is the neutron count rate normalized to a reference atmospheric pressure and solar activity level, N_0 is the count rate over dry soil under the same reference conditions and a_i are fitting parameters. N_0 refers to the neutron production rate and can be determined by adjusting the SWC derived from the CRP to in-situ SWC measurements within the CRP footprint. Using MCNPX simulations for generic silica soils Desilets et al. [2010] derived a_0=0.0808, a_1=0.372 and a_2=0.115 for values of θ>0.02 kg kg^{-1}.

According to Zreda et al. (2008) the size of the horizontal footprint has a radius of about 330 m which is almost independent of SWC. In contrast the measurement depth is strongly dependent on SWC (~75 cm for dry soils and ~12 cm for wet soils).

The effective measurement depth can be expressed by [Franz et al., 2012]:

$$z^* = 5.8\,(\theta + 0.0829)^{-1} \qquad \text{Eq. (2)}$$

where z* is the effective sensor depth [cm] and θ is the soil water content [kgkg^{-1}].

Unfortunately, hydrogen is not only present as SWC. There are additional hydrogen pools that can be separated in approximately static pools (e.g. lattice water, biomass) and dynamic hydrogen pools (e.g. intercepted water in canopy and/or forest floor, surface water, water vapor). In the case that the additional hydrogen in these pools is constant over time, the fast neutron count rate is reduced but this can be accounted for in Eq. 2. However, changing hydrogen content in the dynamic pools within the footprint directly translates in variations in the SWC estimated by the CRP, which affects the measurement accuracy if not properly accounted for. It might even produce unrealistically high SWC estimates that exceed the porosity of the soil, for example when snow or ponded water is present in the footprint. In the context of soil water content monitoring, this is a weakness of the CRP method because it cannot be used in periods with snow cover. In this study, the following hydrogen pools are considered in addition to hydrogen in water: lattice water, organic matter, and root biomass. In order to account for these pools we define a parameter H_p as follows:

$$\mathrm{H}_p = \rho_{bd}(\tau + \lambda + \beta) \qquad \text{Eq. (3)}$$

in which τ, λ and β are the weight fractions of hydrogen in lattice water, hydrogen in organic matter, and hydrogen in root biomass, respectively. These additional hydrogen pools can be considered in Eq. 2 with:

$$z^* = 5.8\,(\theta + H_p + 0.0829)^{-1} \qquad \text{Eq. (4)}$$

Tab. 1 lists average soil properties of the Wüstebach site, which were used to calculate the water weight fractions of the different hydrogen pools (only the top 30 cm was considered since the SWC during the study period never fall below 20 Vol.%).

Table 1: Soil properties of the Wüstebach site

Depth [cm]	Organic matter [w/w]	Organic matter [kg/m²]	Particle density [g/cm³]	Bulk density [g/cm³]	Porosity [%]	Lattice water [kg/m²]	Root biomass [kg/m²]
+5-0 (soil litter)	100	4.58	0.74	0.09	87.63	-	-
0-5	31.65	6.20	2.05	0.39	80.84	0.51	1.000
5-10	11.95	3.90	2.42	0.65	73.04	1.29	0.774
10-15	8.16	3.39	2.49	0.83	66.69	1.90	0.599
15-20	4.32	2.17	2.57	1.01	60.79	2.44	0.463
20-25	3.03	1.56	2.59	1.03	60.33	2.35	0.358
25-30	2.78	1.57	2.60	1.13	56.58	2.54	0.277

Fig. 2 illustrates how the effective sensor depth decreases with increasing SWC and increasing number of hydrogen pools. For dry conditions z* decreases from 70 cm without considering additional hydrogen pools to less than 40 cm for the case that all hydrogen pools are included. Towards wetter conditions the effect of the additional hydrogen pools decreases significantly, so that for very wet soil conditions (e.g. 70 Vol.%) the difference is negligible.

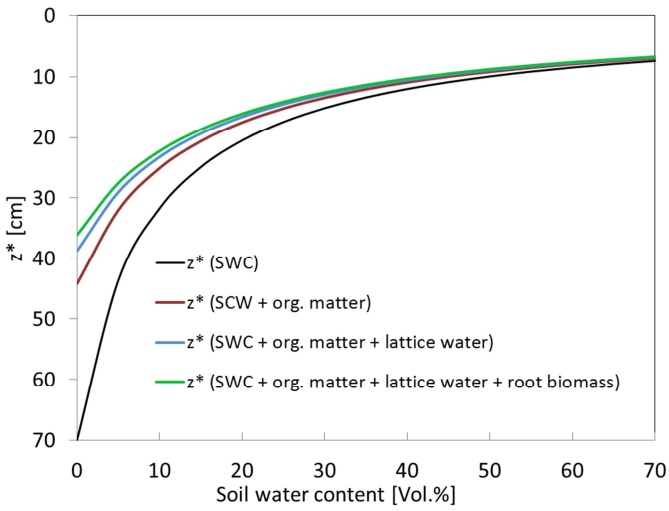

Figure 3: The effective sensor depth versus soil water content and different hydrogen pool combinations.

3.4 Hydrogen pool of the litter layer

The hydrogen pool of the litter layer of the Wüstebach site can account for more than 20 % of the total hydrogen in the footprint of the CRP when the litter layer is saturated (Metzen, 2012). Unfortunately, no continuous measurements of the water dynamics in the litter are available for the study period. Therefore, we used a numerical solution of the one-dimensional Richards equation as implemented in the HYDRUS 1-D software [Simunek et al., 2008] to simulate water dynamics in the litter layer. Soil hydraulic properties were parameterized using the Mualem-van Genuchten model:

$$\theta(h) = \begin{cases} \theta_r + \frac{\theta_s - \theta_r}{[1+|\alpha h|^n]^m} & h < 0 \\ \theta_s & h \geq 0 \end{cases} \qquad \text{Eq. (4)}$$

$$K(h) = K_s S_e^{0.5}\left[1-\left(S_e^{l/m}\right)^m\right]^2 \qquad \text{Eq. (5)}$$

$$S_e = \frac{\theta-\theta_r}{\theta_s-\theta_r} \qquad \text{Eq. (6)}$$

$$m = 1 - 1/n \qquad n > 1 \qquad \text{Eq. (7)}$$

The Mualem-van Genuchten parameters θ_r, α, n, and K_s were inversely estimated from the mean SWC at 5, 20, and 50 cm determined from 600 Soilnet sensors within the CRP footprint for a typical soil profile in the Wüstebach test site (Fig. 4) using the global optimisation scheme SCE-UA [Duan et al., 1992]. The saturated water content θ_s was fixed to the maximum measured soil water content during the study period.

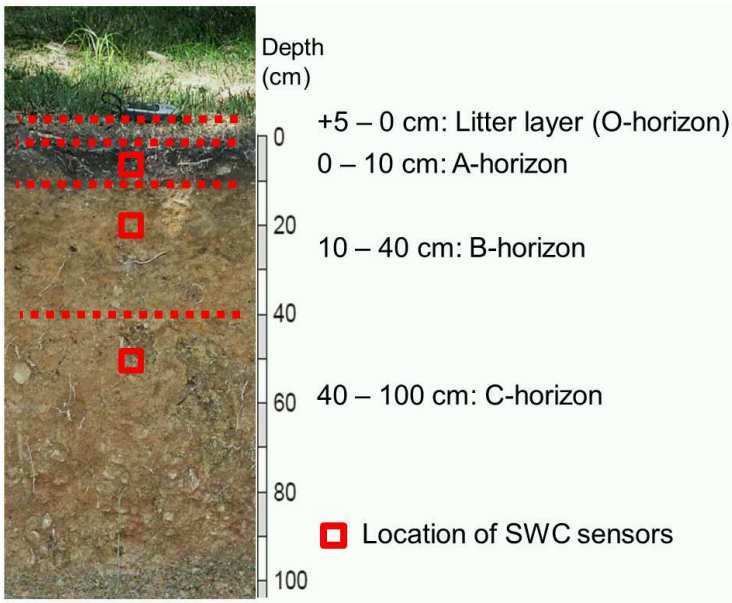

Figure 4: Typical soil profile in the Wüstebach test site and the vertical location of the in-situ soil water content sensors.

We discretised the soil profile in HYDRUS-1D into four materials according to the layering of the typical soil profile. For the parameter estimation, we used SoilNet data from July 1, 2009 to October 31, 2012. Due to the lack of SWC data for the litter layer, the Mualem-van Genuchten parameters proposed by Schaap et al. (1997) were used for this layer. In addition, the mean porosity of eight litter layer samples was used to parameterize θ_s of the litter layer.

Table 2: Optimized soil hydraulic properties (black letters), parameters of Schaap et al. (1997) (red letters), and measured saturated water content (green letters).

	Θ_r	Θ_s	α	n	K_s [cm/h]
O	0	0.87	0.0254	1.286	200
Aeh	0.1802	0.57	0.002681	1.411	125.5
Bv-Sw	0.1976	0.4879	0.002525	1.305	271.9
Sd	0.1338	0.38	0.001053	1.322	3.238

3.5 Comparison of cosmic ray with in-situ data

To enable a comparison of the SWC information from SoilNet with the CRP data, the in-situ measurements of SoilNet need to be vertically and horizontally weighted to account for the instrument response of the CRP. In this study, we use empirical weighting functions that were developed on the basis of neutron transport simulation results using the MCNP code [Zreda et al., 2008]. According to this study, the horizontal footprint is independent of SWC and the weights can thus be directly derived from the numerical simulations. However, since the sensor depth is strongly dependent on the SWC, this has to be accounted for in the weighting procedure. In order to do so, we selected an empirical function to describe the relationship between cumulative counts (CFoC) and depth (z) published by Zreda et al. [2008] for two soil water contents:

$$z = -\alpha \cdot ln(1 - CFoC) \qquad \text{Eq. (5)}$$

The CFoC can be used to calculate the vertical weights (W_z) required to link the SoilNet and CRP data. The empirical functions fitted to the data of Zreda et al., [2008] are shown in Fig. 5:

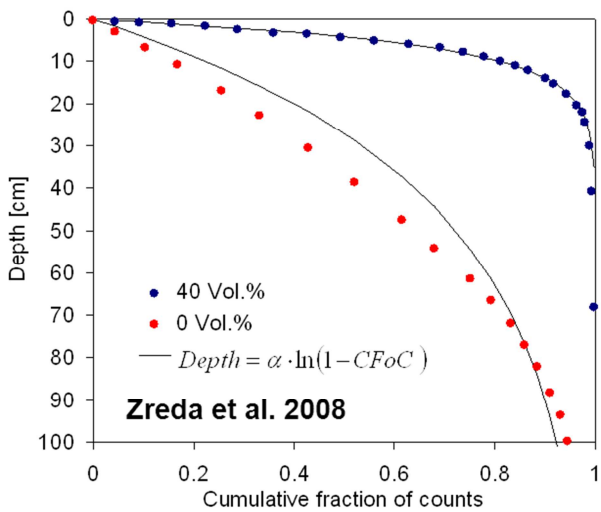

Figure 5: The fitted functions of the theoretical modelled sensing depths by Zreda et al. (2008).

According to Franz et al. [2012] the two e-folding sampling volume is defined as the volume within which 86% of the detected neutrons above the surface originate. Therefore the effective depth of the cosmic ray probe z* is defined as the 86% cumulative sensitivity point:

$$z^* = -\alpha \cdot ln(1 - 0.86) \qquad \text{Eq. (8)}$$

Combining Eq. 4 and Eq. 7 yields a direct relationship between α and soil water content:

$$\alpha = \frac{-5.8}{ln(0.14) \cdot (\theta + H_p 0.0829)} \qquad \text{Eq. (9)}$$

By rearranging Eq. 7 the vertical weight w_z can be calculated for different depths and α values:

$$CFoC = 1 - e^{\left(-\frac{z}{a}\right)} \qquad \text{Eq. (10)}$$

$$w_z = CFoC' = \frac{d}{dz} e^{\left(-\frac{z}{a}\right)} \cdot \frac{1}{a} \qquad \text{Eq. (11)}$$

We used an iterative calculation procedure to derive the vertical weights for each sensor depth. First, the vertical average of the measured SWC profile is used to obtain an approximate estimate of the weights. The deepest layer for which SWC information is available contributes the remaining weight towards 100% of the cumulative fraction of counts. In the next step, a new estimate of the weighted average SWC is calculated using the approximate weights. This procedure is repeated until the change in updated weighted averaged SWC is negligible (< 0.01 Vol.%). Typically, five iterations were sufficient.

4 Results

4.1 Comparison of cosmic ray with in-situ SoilNet data

We used the weighted averaged SoilNet data to calibrate the CRP calibration function (Eq. 1) for the estimation of SWC from the measured fast neutron count rates. As suggested by Desilets et al. [2010], we only calibrated the parameter N_0. In addition, we excluded time periods with snow from the calibration. The result is shown in Fig. 5.

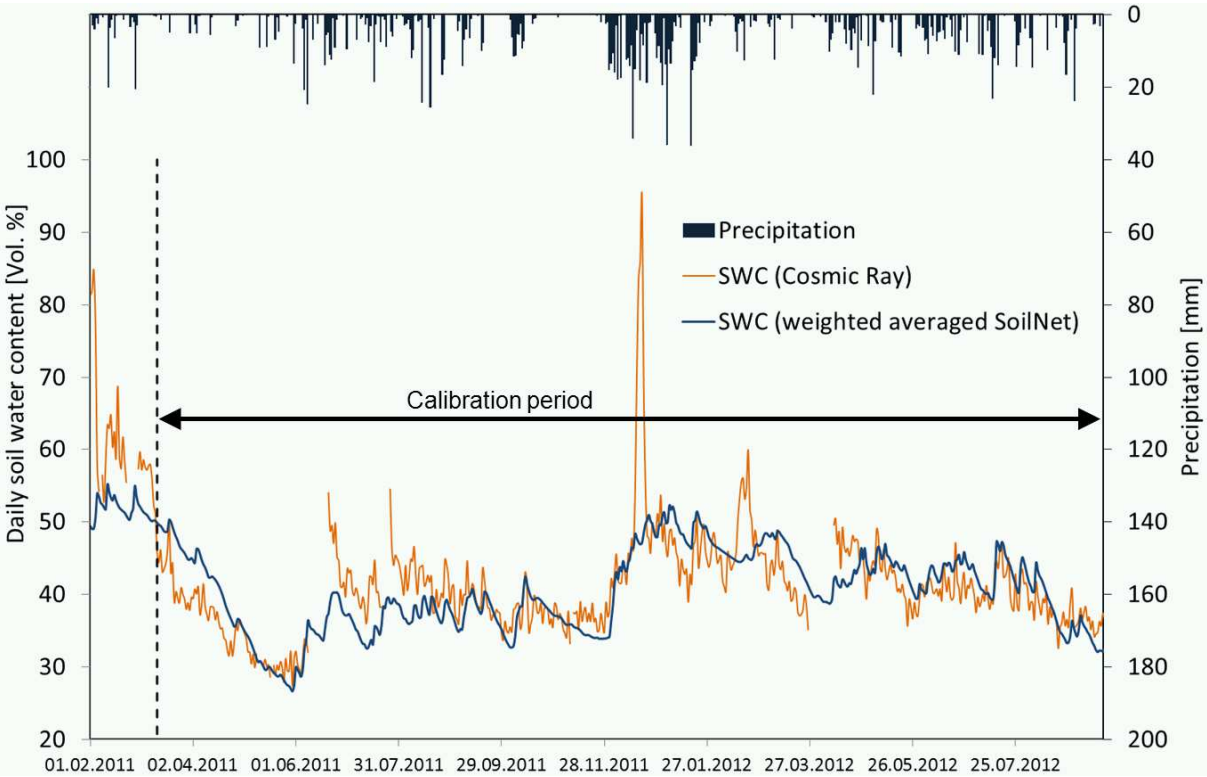

Figure 6: Cosmic ray SWC time series derived from calibration using SoilNet data versus the weighted averaged soil water content as measured by SoilNet.

The calibration resulted in a RMSE of 3.66 Vol.%, which is comparable to the measurement uncertainty of the in-situ electromagnetic SWC sensors used in the sensor network.

However, there are also some larger deviations between the two SWC time series. In particular, a significant overestimation of SWC is visible during four days in December 2011. This can be attributed to a thick snow cover, which depresses the fast neutron intensity. Fig. 7 shows the effect of snow on the estimated SWC from the fast neutron count rates in greater detail.

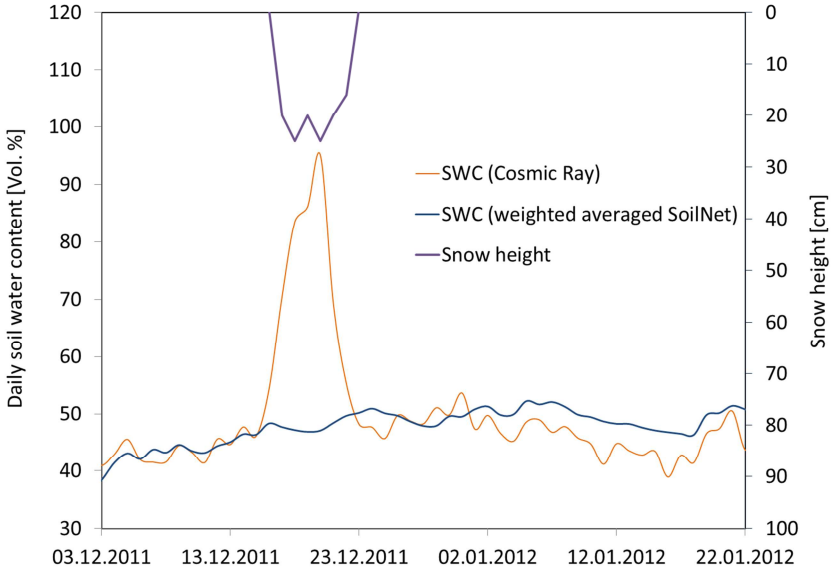

Figure 7: The effect of snow cover on the soil water content measurements using the CRP.

During four days with snow, the estimated SWC exceeded the expected values by more than 40 Vol.%. According to Desilets et al. (2010), this effect can potentially be used to estimate the snow cover depth from the CRP measurements. However, since an appropriate method is still not available, more research is needed to come up with appropriate estimates of average snow depths from CRP data.

4.2 Modelled water dynamics of the litter layer

As explained earlier, no water content measurements of the litter layer were available for this study period. Therefore we used the HYDRUS-1D model to generate continuous water contents of the litter layer. Fig. 6 shows the observed and simulated soil water contents in 5, 20 and 50 cm depth as well as the simulated water dynamics of the litter layer. After optimising the hydraulic parameters, the HYDRUS-1D model was able to reproduce the soil water contents dynamics at 5, 20 and 50 cm depth in a reasonable way (RMSE were 3.65, 2.0 and 1.52 Vol.%, respectively).

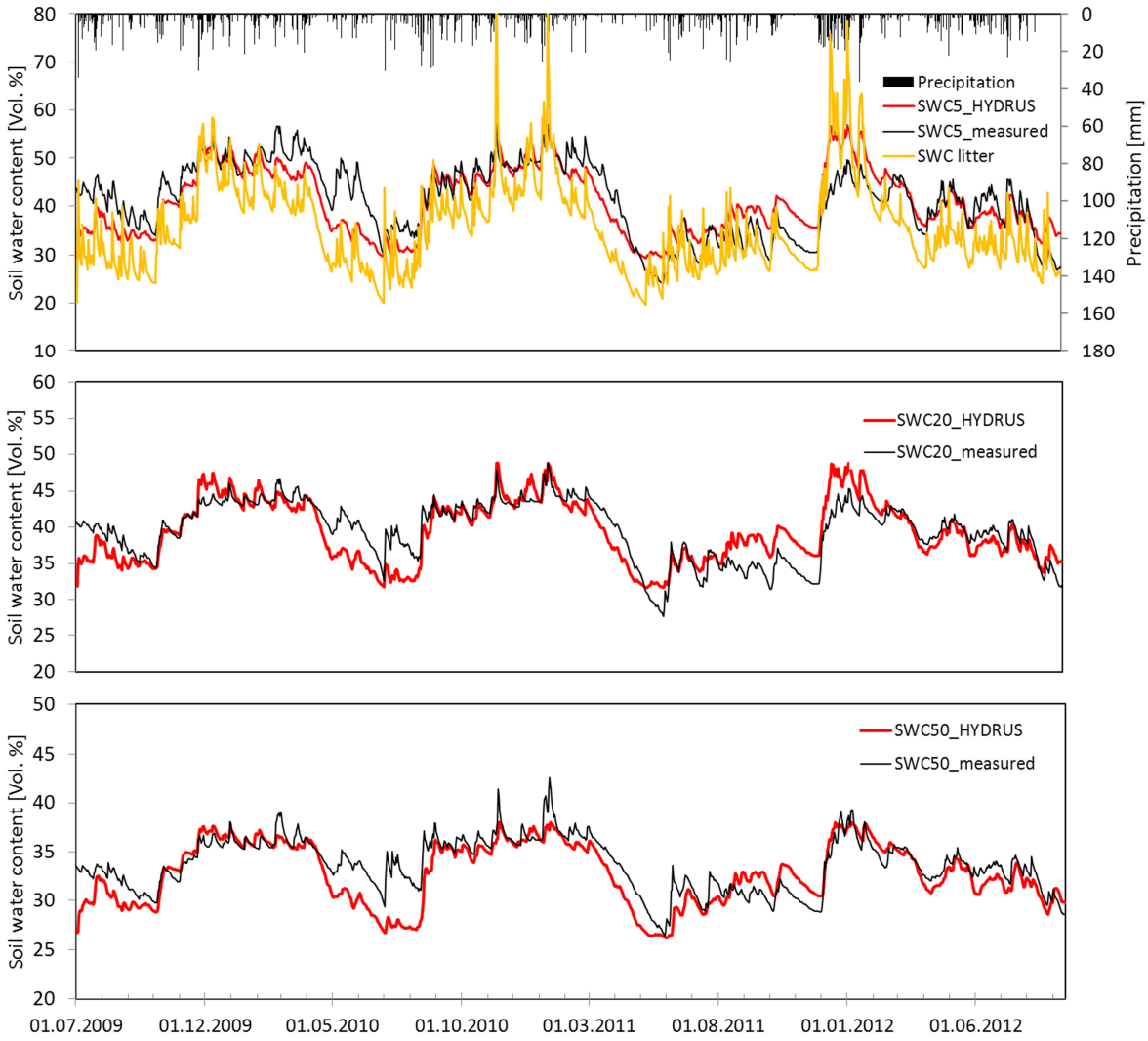

Figure 8: Observed versus simulated soil water contents in 5, 20 and 50 cm depth as well as the simulated water dynamics of the litter layer.

As expected, the water content of the litter layer shows higher temporal dynamics than the soil water content in 5 cm, which is mainly due to the lower *n* value we used from the paper of Schaap et al. (1997). Although we do not have data to validate the simulated water dynamics, we feel that this information is appropriate enough to analyse the effect of the litter layer on the neutron count rate.

4.3 Comparison of cosmic ray with in-situ SoilNet data and modelled water dynamics of the litter layer

As indicated before, the hydrogen pool of the litter layer affects the emission of fast neutron from the soil. Therefore, we included the simulated water content of the litter layer in the vertical averaging of the soil water content profile. The result of this new calibration is presented in Fig. 9.

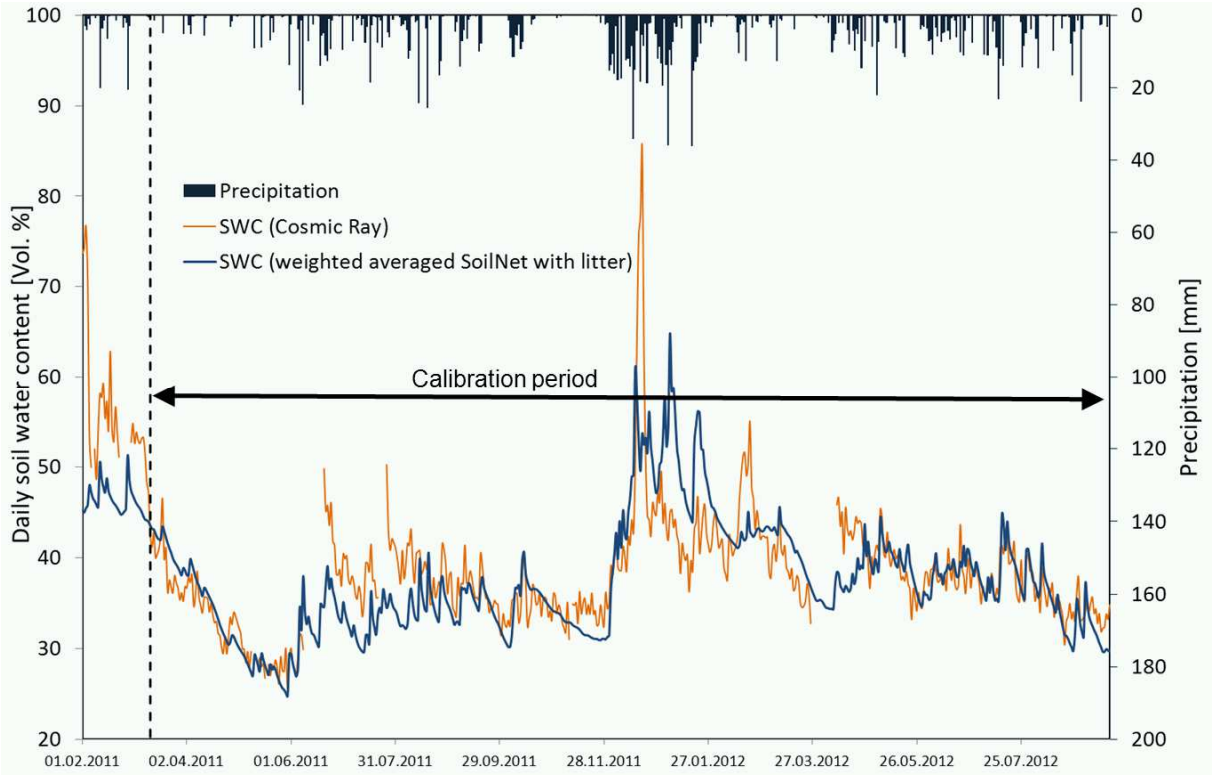

Figure 9: Cosmic ray SWC time series derived from calibration using SoilNet data and simulated water dynamics of the litter layer versus the weighted averaged SoilNet SWC.

The new calibration resulted in a RMSE of 2.92 Vol.%, which is 0.74 Vol.% lower than without considering the water dynamics of the litter layer. This indicates that dynamics of the hydrogen pool in the litter layer affect the fast neutron emission and thus should be considered in the calibration when CRP are used in forest ecosystems.

5 Conclusion

Data from a wireless soil moisture sensor network were used to evaluate the applicability of the cosmic ray method for measuring soil water content in forests with a litter layer.

The results of this study have led us to the following conclusions:

- The newly developed vertical weighting function enables the comparison of the sensor network data with the water content estimates of the cosmic ray probe
- The use of in-situ soil water content data from a wireless sensor network resulted in a successful calibration of the cosmic ray probe
- Including simulated water contents of litter layer in the calibration provided better calibration results

The take-home message from this study is that static and dynamical hydrogen pools need to be considered for reliable soil moisture estimations using cosmic ray probes.

6 References

Bogena, H. R., M. Herbst, J. A. Huisman, U. Rosenbaum, A. Weuthen, and H. Vereecken (2010), Potential of wireless sensor networks for measuring soil water content variability, Vadose Zone J., 9(4), 1002–1013, doi:10.2136/vzj2009.0173.

Desilets, D. & M. Zreda (2001): On scaling cosmogenic nuclide production rates for altitude and latitude using cosmic ray measurements. Earth Planet. Sci. Lett. 193.

Desilets, D., M. Zreda, and T. P. A. Ferre (2010), Nature's neutron probe: Land surface hydrology at an elusive scale with cosmic rays, Water Resour. Res., 46, W11505, doi:10.1029/2009WR008726.

Dorman, L. (2004): Cosmic rays in the earth's atmosphere and underground. Kluwer Academic Publishers, Dordrecht.

Duan, Q., Sorooshian, S. & Gupta, V. (1992): Effective and efficient global optimization for conceptiual rainfall-runoff models. W. Resour. Res., 28: 4, 1015-1031.

Etmann, M. (2009): Dendrologische Aufnahmen im Wassereinzugsgebiet Oberer Wüstebach anhand verschiedener Mess- und Schätzverfahren. Master thesis. University of Münster.

Franz, T. E., M. Zreda, T. P. A. Ferre, R. Rosolem, C. Zweck, S. Stillman, X. Zeng, and W. J. Shuttleworth (2012): Measurement depth of the cosmic ray soil moisture probe affected by hydrogen from various sources, Water Resour. Res., 48, doi:10.1029/2012WR011871.

Gaisser, T.K. (1990): Cosmic Rays and Particle Physics. Cambridge Univ. Press, Cambridge.

Hendrick, L.D. & R.D. Edge (1966): Cosmic-ray neutrons near the earth. Phys. Rev. 145.

Hess, W.N., Canfield, E.H. & R.E. Lingenfelter (1961): Cosmic-Ray Neutron Demography. J. Geophys. Res. 66.

Lal, D. & B. Peters (1967): Cosmic ray produced radioactivity on the earth. In: Sitte, K. (Ed.): Handbuch der Physik. Springer-Verlag, Berlin.

Metzen, D. (2012): Capability of the Cosmic Ray Sensor for the assessment of mesoscale soil moisture variability in the catchment of the Rur River. Master thesis. Geographisches Institut der Rheinischen Friedrich-Wilhelms-Universität Bonn.

Parker, E.N. (1965): The passage of energetic charged particles through interplanetary space. Planet. Space Sci. 13: 9-49.

Phillips, F. M., Stone, W. D. & J. T. Fabryka-Martin (2001): An improved approach to calculating low-energy cosmic-ray neutron fluxes near the land/atmosphere interface. Chem. Geol. 175.

Richter, F. (2008), Bodenkarte zur Standorterkundung. Verfahren Quellgebiet Wüstebachtal (Forst). Geol. Dienst Nordrhein-Westfalen, Krefeld, Germany.

Rivera Villarreyes, C.A., Baroni, G. & S.E. Oswald (2011): Integral quantification of seasonal soil moisture changes in farmland by cosmic-ray neurons. Hydrol. Earth Syst. Sci. 15:3843-3859.

Rosenbaum, U., H. R. Bogena, M. Herbst, J. A. Huisman, T. J. Peterson, A. Weuthen, A. W. Western, and H. Vereecken (2012), Seasonal and event dynamics of spatial soil moisture patterns at the small catchment scale, Water Resour. Res., 48, W10544, doi:10.1029/2011WR011518.

Rosenbaum, U., J. A. Huisman, A. Weuthen, H. Vereecken, and H. R. Bogena (2010), Sensor-to-sensor variability of the ECH2O EC-5, TE, and 5TE sensors in dielectric liquids, Vadose Zone J., 9, 181–186, doi:10.2136/vzj2009.0036.

Simunek, J., M. T. van Genuchten, and M. Sejna (2008): Development and applications of the HYDRUS and STANMOD software packages and related codes, Vadose Zone J., 7(2), 587–600, doi:10.2136/Vzj2007.0077.

Zacharias, S., et al. (2011), A network of terrestrial environmental observatories in Germany, Vadose Zone J., 10, 955–973, doi:10.2136/vzj2010.0139.

Zreda, M., Desilets, D., Ferré, T.P.A. & R.L. Scott (2008): Measuring soil moisture content non-invasively at intermediate spatial scale using cosmic-ray neutrons. Geophys. Res. Lett. 35.

Zreda, M., W. J. Shuttleworth, X. Xeng, C. Zweck, D. Desilets, T. E. Franz, R. Rosolem, and P. A. Ferre (2012), COSMOS: The COsmic-ray Soil Moisture Observing System, Hydrology and Earth System Sciences, 16, 4079-4099. doi:10.5194/hess-16-1-2012.